

Supporting Information

for

Quantification of Electrogenenerated Chemiluminescence from Tris(bipyridine)ruthenium(II) and Hydroxyl Ions

Andrea Fiorani[†], Giovanni Valenti[‡], Irkham[†], Francesco Paolucci[‡], and Yasuaki Einaga^{†}*

[†]Department of Chemistry, Keio University, 3-14-1 Hiyoshi, Yokohama 223-8522, Japan

[‡]Department of Chemistry “G. Ciamician”, University of Bologna, Via Selmi 2, 40126 Bologna,
Italy

Contents	Page
Figure S1. Cyclic voltammetry at different pH for perchlorate and phosphate	S3
Figure S2. CV-ECL, cyclic voltammetry, and integrated ECL at different pH in carbonate	S4
Figure S3. Comparison of Ru(bpy) ₃ ²⁺ ECL with NaOH and tri- <i>n</i> -propylamine	S5
Figure S4. Effect of electrode material (GC and BDD) on ECL emission	S6
Figure S5. Effect of counter electrode and oxygen on ECL emission	S7
Figure S6. ECL emission spectra	S8
Part 1: The catalytic constant (k_{OH}) of reaction in Scheme 1 and TOF- η relationship	S8
Figure S7. Cyclic voltammetry of Ru(bpy) ₃ ²⁺ and Ru(bpy) ₃ ²⁺ /NaOH	S8
Figure S8. Foot of the wave analysis	S10
Figure S9. Cyclic voltammetry comparison with foot of the wave analysis	S11
Part 2: Mechanism and energetic considerations	S11
References	S12

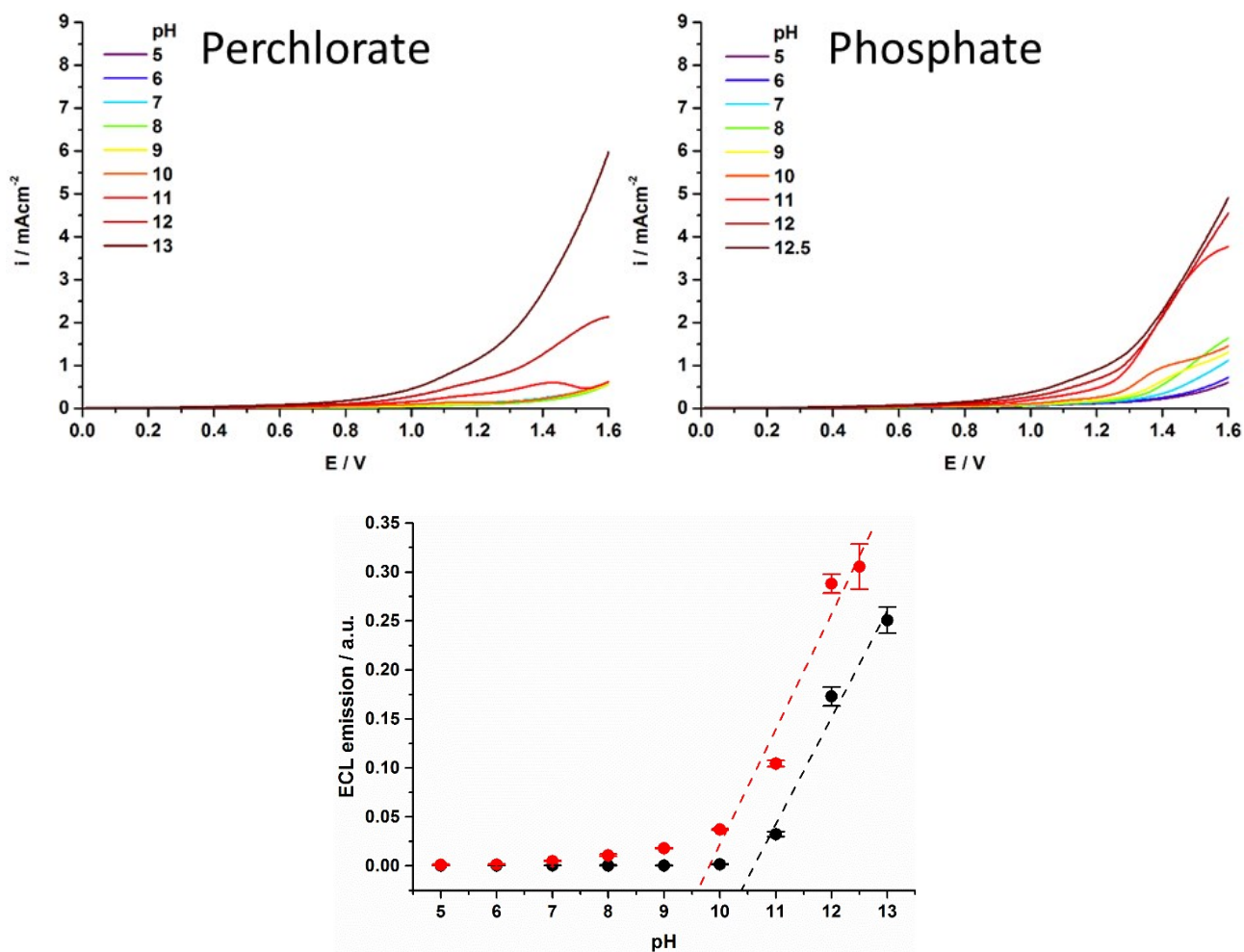


Figure S1. (Top) Current of forward scan of CV-ECL (for Fig. 1, main text) at different pH for the 100 mM electrolytes. Scan rate is 100 mVs^{-1} . Potential referred to Ag/AgCl (saturated KCl). (Bottom) Linear fitting of the ECL emission vs pH (from Fig. 2, main text).

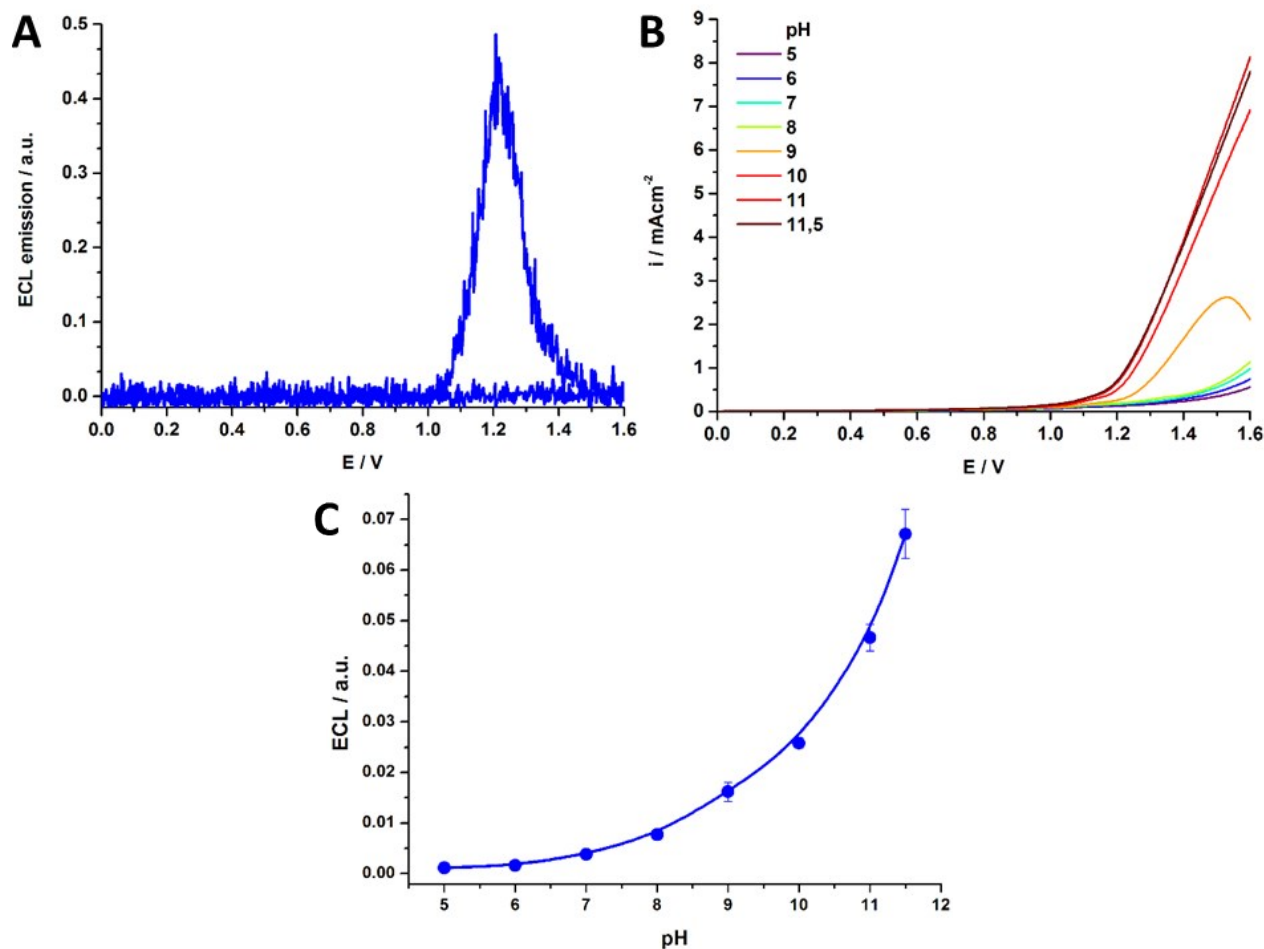


Figure S2. A) ECL emission of 100 μM $\text{Ru}(\text{bpy})_3^{2+}$ in 100 mM carbonate pH 11.5 at 100 mVs^{-1} , and B) current of forward scan from CV-ECL at different pH. Scan rate is 100 mVs^{-1} . Potential referred to Ag/AgCl (saturated KCl). C) Integrated ECL emission from cyclic voltammetry at different pH. The line is drawn only as guide for the eye.

The ECL with carbonate differs from perchlorate and phosphate, its emission starts at the same time of others electrolytes, concurrently with $\text{Ru}(\text{bpy})_3^{2+}$ oxidation, but it features only a single peak that gives a lower ECL emission (Figure S2-A).

Carbonate oxidation might hinder the ECL emission in competition with the oxidation process of $\text{Ru}(\text{bpy})_3^{2+}$.

The current measured for carbonate is four and two times higher than perchlorate and phosphate, respectively (Figure S1 and S2-B).

Carbonate can be oxidized to percarbonate, which later decomposes in hydrogen peroxide.¹ This may lead to competition with Ru(II) oxidation or limiting the availability of hydroxide ions in the diffusion layer, since hydroxide enter the catalytic decomposition of hydrogen peroxide.² Moreover, hydrogen peroxide is a quencher of Ru(II) excited state.³ Another possible reaction pathway, involving hydroxyl radicals, is the extremely rapid addition to Ru(III) ($k_{\text{OH}} = (0.6\text{-}2.0) \times 10^{10} \text{ M}^{-1}\text{s}^{-1}$),⁴ that will scavenge the Ru(III) preventing further reaction with OH⁻.

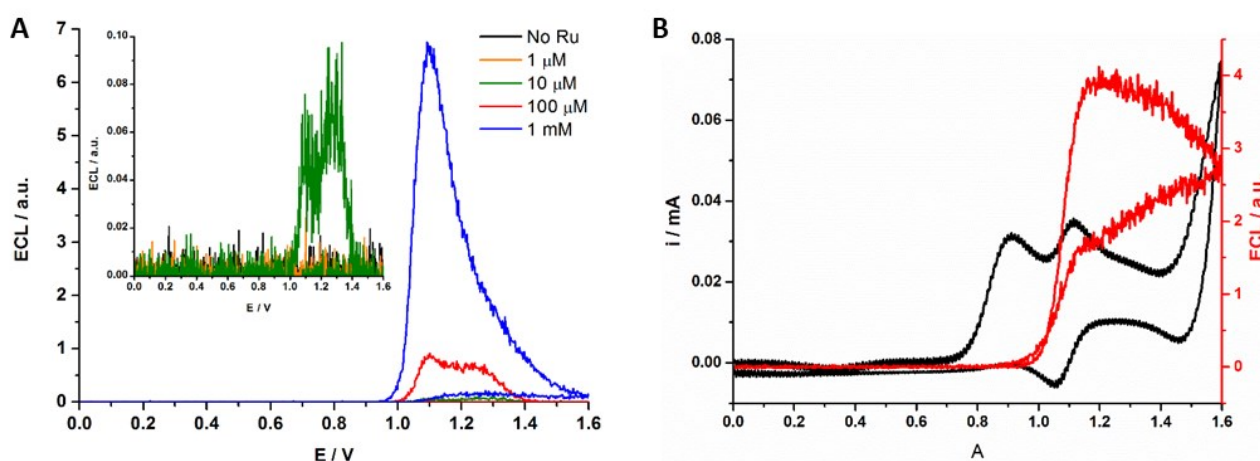


Figure S3. A) CV-ECL for different concentration of Ru(bpy)₃²⁺ in 1 M NaOH at 100 mVs⁻¹. B) CV-ECL of 100 μM Ru(bpy)₃²⁺ and 100 μM tri-*n*-propylamine in 0.2 M phosphate buffer (pH 7.5) at 100 mVs⁻¹ (CV is background subtracted).

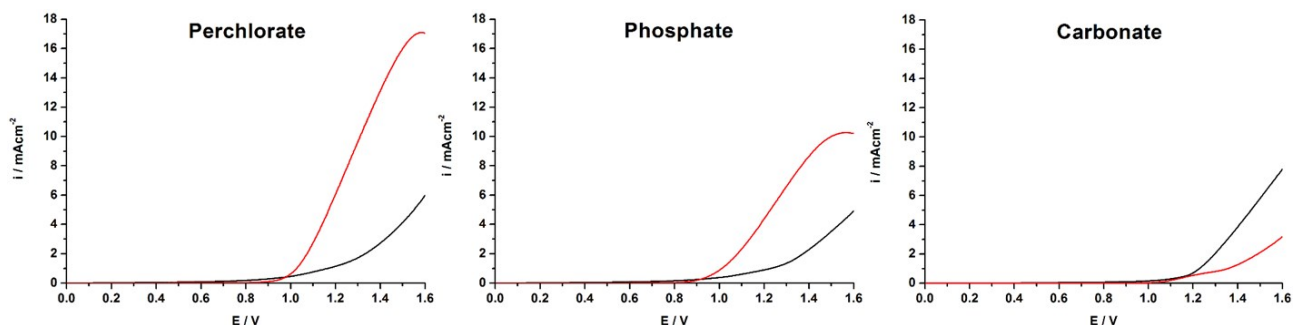
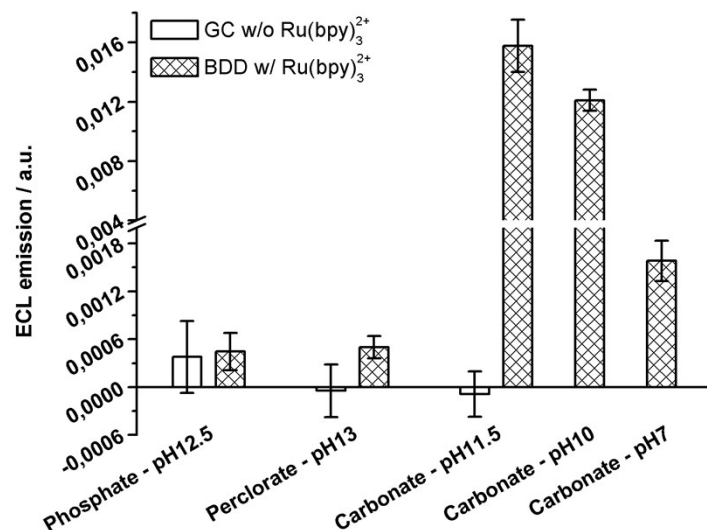


Figure S4. Top: integrated ECL signal from CV-ECL, GC without (GC w/o Ru(bpy)₃²⁺) and BDD with (BDD w/ Ru(bpy)₃²⁺) 100 μM Ru(bpy)₃²⁺ in 100 mM supporting electrolyte at the specified pH. Bottom: current of forward scan from CV-ECL at 100 mM electrolytes with Ru(bpy)₃²⁺ 100 μM (BDD, red line; GC, black line). Scan rate is 100 mVs⁻¹. Potential referred to Ag/AgCl (saturated KCl).

For perchlorate and phosphate electrolytes, the current measured with BDD electrode is oxidation of hydroxyl anions,^{5,6} and it is higher than current measured for GC. This results in the depletion of hydroxyl ions at BDD and quenching of the ECL emission, while a detectable ECL emission is retained with carbonate that shows a lower current for BDD than GC.

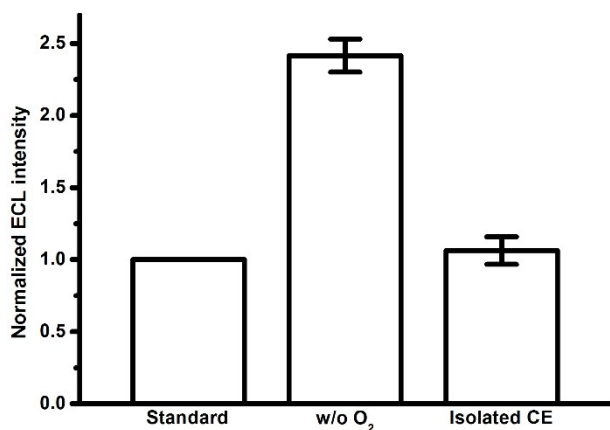


Figure S5. Normalized ECL intensity of the ECL system in the three electrode configuration (standard), without oxygen (10 ml of solution bubbled for 30 min with 20 ml/min nitrogen stream), and with isolated counter electrode (inside a glass tube closed with Vycor porous glass and filled with the electrolytic solution). Ru(bpy)₃²⁺ 100 μM, phosphate 100 mM (pH 12.5); cyclic voltammetry from 0 V to 1.6 V at 100 mV/s. Error bar for the standard configuration is smaller than bar lines.

The increase of emission after nitrogen bubbling is ascribed to the quenching effect of oxygen on the excited state of Ru(bpy)₃^{2+*}.⁷ The same emission obtained with isolated counter electrode rule out any parasitic reaction that may generate ECL at the counter electrode and might be wrongly associated with the main ECL system here investigated.⁸

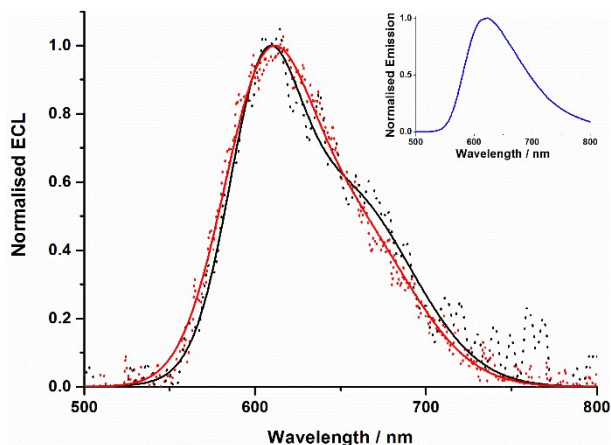


Figure S6. Normalised spectra: ECL emission for 1 mM Ru(bpy)₃²⁺ with 1M NaOH (black, $\lambda_{\text{max}} = 610$ nm), and 100 μM Ru(bpy)₃²⁺ with 100 μM TPrA in phosphate buffer at pH 7.5 (red, $\lambda_{\text{max}} = 612$ nm), obtained by chronoamperometry at 1.4 V on GC and 1.7 V on BDD, respectively; two peaks fitting, Gaussian function. Inset, photoluminescence emission for 50 μM Ru(bpy)₃²⁺ in 100 mM Na₂SO₄ ($\lambda_{\text{max}} = 623$ nm). Spectra are uncorrected.

Part 1: The catalytic constant (k_{OH}) of reaction in Scheme 1 and TOF- η relationship

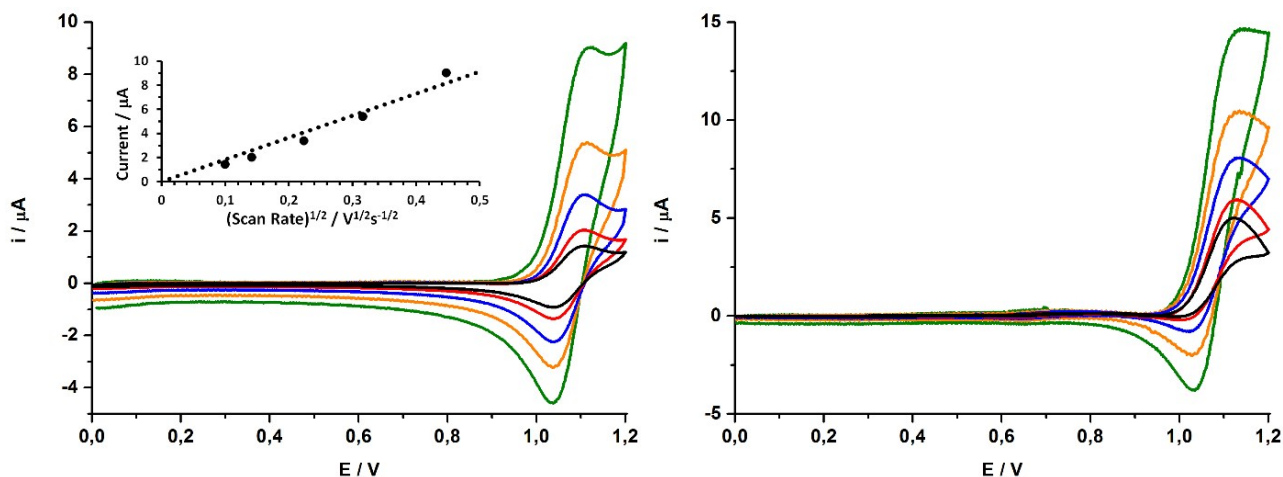


Figure S7. Background subtracted CVs of (left) 0.5 mM Ru(bpy)₃²⁺ in 100 mM Na₂SO₄ (pH 6), and (right) 0.5 mM Ru(bpy)₃²⁺ in 100 mM Na₂SO₄ and 1 mM NaOH. Scan rates at 10, 20, 50, 100 and 200 mV/s. Working electrode is glassy carbon $\varnothing = 3$ mm.

$E_{1/2}^{Ru^{3+/2+}} = 1.07$ V is used in the following foot of the wave analysis and measured from CV experiments (Figure S5, left), in agreement with previous results.⁹

The classical S-shaped catalytic wave follows the equation:

$$i = \frac{FAC_{Ru}^0 \sqrt{D_{Ru}} \sqrt{k_1 C_{OH^-}^0}}{1 + \exp\left[\frac{F}{RT}(E - E_{1/2}^{Ru^{3+/2+}})\right]}$$

The peak current of $Ru(bpy)_3^{2+}$ without NaOH is given by:

$$i_p = 0.446FAC_{Ru}^0 \sqrt{D_{Ru}} \sqrt{\frac{Fv}{RT}}$$

Then, calibration of i for the electrode surface area (A), the catalyst concentration (C_{Ru}^0) and the diffusion coefficient (D_{Ru}) lead to:

$$\frac{i}{i_p} = \frac{2.24 \sqrt{\frac{RT}{Fv}} k_1 C_{OH^-}^0}{1 + \exp\left[\frac{F}{RT}(E - E_{1/2}^{Ru^{3+/2+}})\right]}$$

Plotting this against $1/\{1 + \exp[F/RT(E - E_{1/2}^{Ru^{3+/2+}})]\}$ gives a straight line with slope

$2.24(RT/Fv)^{1/2}(k_1 C_{OH^-}^0)^{1/2}$, to access $k_1 C_{OH^-}^0$ [$M^{-1}s^{-1}$],

as the pseudo-first order rate constant k_{OH} [s^{-1}].^{10,11}

$$TOF = \frac{k_{OH}}{1 + \exp\left[\frac{F}{RT}(E_{1/2}^{Ru^{3+/2+}} - E_{H_2O/O_2} - \eta)\right]}$$

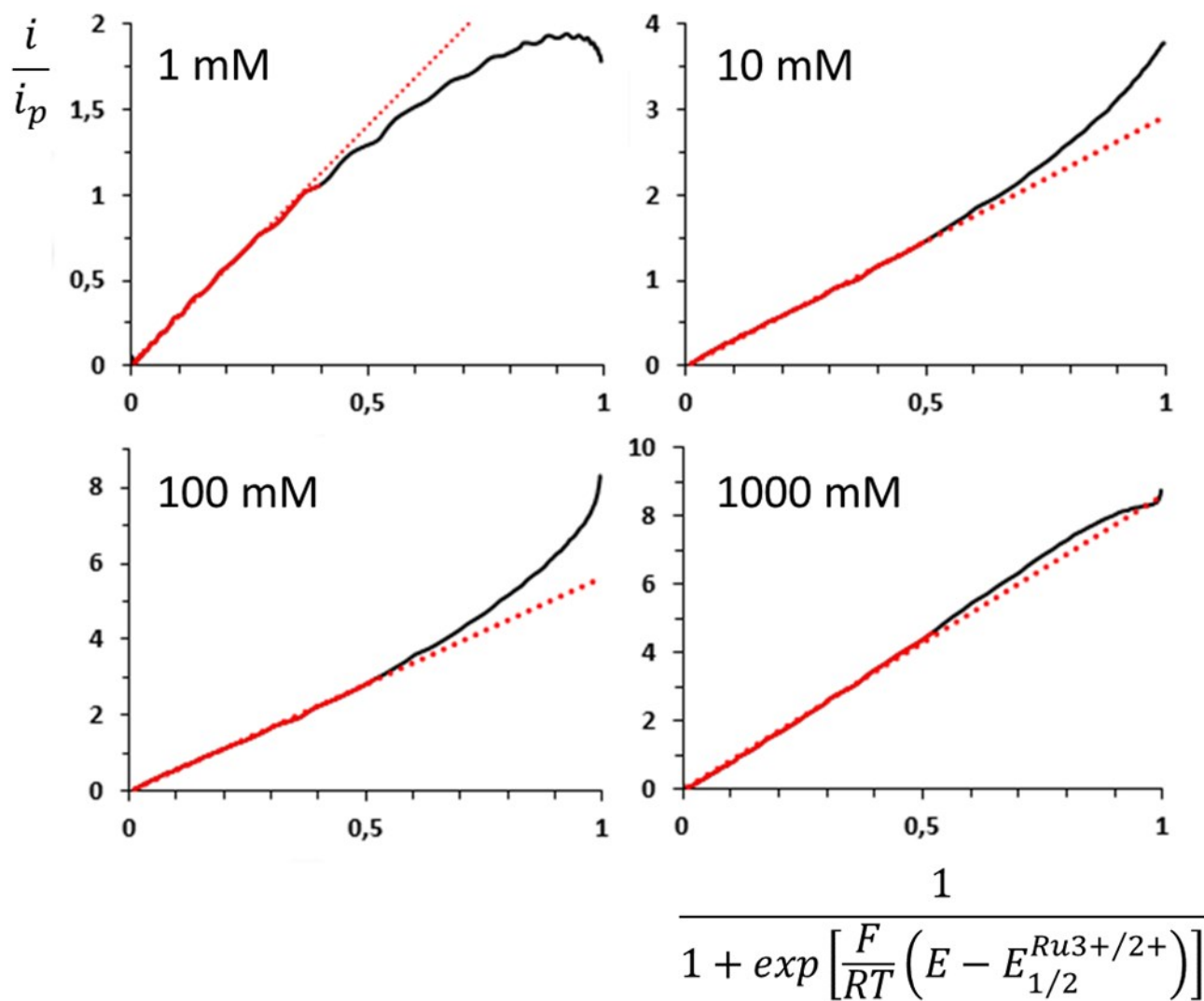


Figure S8. Foot of the wave analysis: CV of 0.5 mM $Ru(bpy)_3^{2+}$ in 100m M Na_2SO_4 and NaOH as specified. Scan rate is 100 mV/s. Glassy carbon $\varnothing = 3$ mm. The y-axis is i/i_p (i_p is the peak current of the CV at 100 mV/s in Figure S5, left), and the x-axis is $1/\{1+\exp[F/RT(E-E_{1/2}^{Ru^{3+}/2+})]\}$.

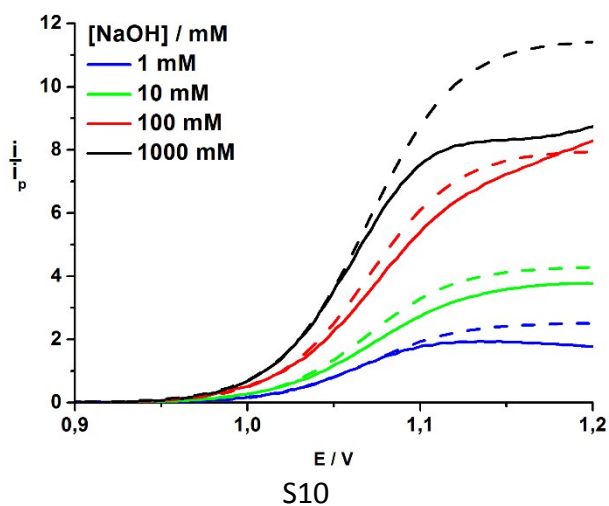


Figure S9. Forward scan CVs (background subtracted) with 0.5 mM Ru(bpy)₃²⁺ and NaOH at specified concentrations in 100 mM Na₂SO₄ at 100 mVs⁻¹ (full line). Fitting from foot of the wave analysis (dashed line).

Part 2: Mechanism and energetic considerations

Investigation of the undelaying mechanism involved in the ECL emissions is not the aim of this study, however we report some previous researches on the reaction mechanism of Ru(III) and OH⁻ to justify the assumptions used for the measurement of TOF. Ru(III) reduction by hydroxyl ions was first studied as potential application in a solar energy storage system, in photochemical water splitting.⁴

This mechanism, as described by Ghosh et al.,¹² and Lay et al.,¹³ sees the first chemical step of this reaction as hydroxide addition on bpy ligand. Further reactions with Ru(III) are considered in the mentioned reaction mechanism, which may be involved in the ECL emission, for a second-order reaction in Ru(III). Furthermore, chemiluminescence from Ru(III) reduction may arise from hydroxyl ion attack at a coordinated bpy followed by intramolecular electron transfer from ligand to metal.¹⁴

Another mechanism, proposed by Serpone et al.,^{15,16} concerns the formation of tight ion-pairs in an outer-sphere complex between the bpy ligands of Ru(III) and OH⁻. This offers also a straightforward interpretation of the chemiluminescence reaction, since it predicts the formation of a MLCT excited stated ($d^5\pi^{*1} \rightarrow d^6$).

Concerning the ECL mechanism, we want to point out, the free Gibbs energy (ΔG_{es})¹⁷ for the formation of the excited state (Ru^{2+*}, ³MLCT = 2.12 eV)¹⁸ is unfavourable, since the energy available from direct water oxidation is not sufficient.

$$\Delta G_{es} \simeq E_{O_2/H_2O}^0(pH\ 12) - E_{Ru(bpy)_3^{2+}}^0 + \frac{1}{2} + {}^3MLCT Ru(bpy)_3^{2+} = 1.37\text{eV} \quad (3)$$

Moreover, one electrode oxidation of OH^- to OH^\bullet is not possible on energetic ground,¹³ because the formation of $^3\text{MLCT}^* \text{Ru(II)}$ and OH^\bullet is endoergonic of about 3 eV.

REFERENCES

- (1) Zhang, J.; Oloman, C. W. Electro-Oxidation of Carbonate in Aqueous Solution on a Platinum Rotating Ring Disk Electrode. *J. Appl. Electrochem.* **2005**, *35*, 945-953.
- (2) Duke, F. R.; Haas, T. W. The homogeneous base-catalyzed decomposition of hydrogen peroxide. *J. Phys. Chem.* **1961**, *65*, 304-306.
- (3) Choi, J.-P.; Bard, A. J. Electrogenenerated chemiluminescence (ECL) 79. Reductive-oxidation ECL of tris(2,2'-bipyridine)ruthenium(II) using hydrogen peroxide as a coreactant in pH 7.5 phosphate buffer solution. *Anal. Chim. Acta* **2005**, *541*, 143-150.
- (4) Creutz, C.; Sutin, N. Reaction of tris(bipyridine)ruthenium(III) with hydroxide and its application in a solar energy storage system. *Proc. Nat. Acad. Sci. USA* **1975**, *72*, 2858-2862.
- (5) Irkham; Watanabe, T.; Einaga, Y. Hydroxide Ion Oxidation in Aqueous Solutions Using Boron-Doped Diamond Electrodes. *Anal. Chem.* **2017**, *89*, 7139-7144.
- (6) Irkham; Einaga, Y. Oxidation of hydroxide ions in weak basic solutions using boron-doped diamond electrodes: effect of the buffer capacity. *Analyst*, **2019**, *144*, 4499-4504.
- (7) Mulazzani, Q. G.; Sun, H.; Hoffman, M. Z.; Ford, W. E.; Rodgers, M. A. J. Quenching of the Excited States of Ruthenium(II)-Diimine Complexes by Oxygen. *J. Phys. Chem.* **1994**, *98*, 1145-1150.
- (8) Theakstone, A. G.; Doeven, E. H.; Conlan, X. A.; Dennany, L.; Francis, P. S. 'Cathodic' electrochemiluminescence of $[\text{Ru}(\text{bpy})_3]^{2+}$ and tri-n-propylamine confirmed as emission at the counter electrode. *Chem. Commun.* **2019**, *55*, 7081-7084.
- (9) Miao, W.; Choi, J.-P.; Bard, A.J. Electrogenenerated Chemiluminescence 69: The

-
- Tris(2,2'-bipyridine)ruthenium(II), (Ru(bpy)₃²⁺)/Tri-*n*-propylamine (TPrA) System Revisited-A New Route Involving TPrA⁺ Cation Radicals. *J. Am. Chem. Soc.* **2002**, *124*, 14478-14485.
- (10) Costentin, C.; Drouet, S.; Robert, M.; Savéant, J.-M. Turnover Numbers, Turnover Frequencies, and Overpotential in Molecular Catalysis of Electrochemical Reactions. Cyclic Voltammetry and Preparative-Scale Electrolysis. *J. Am. Chem. Soc.* **2012**, *134*, 11235-11242.
- (11) Correction to Costentin, C.; Drouet, S.; Robert, M.; Savéant, J.-M. Turnover Numbers, Turnover Frequencies, and Overpotential in Molecular Catalysis of Electrochemical Reactions. Cyclic Voltammetry and Preparative-Scale Electrolysis. *J. Am. Chem. Soc.* **2012**, *134*, 19949-19950.
- (12) Ghosh, P. K.; Brunschwig, B. S.; Chou, M.; Creutz, C.; Sutin, N. Thermal and light-induced reduction of the ruthenium complex cation Ru(bpy)₃³⁺ in aqueous solution. *J. Am. Chem. Soc.* **1984**, *106*, 4772-4783
- (13) Lay, P. A.; Sasse, W. H. F. Mechanism of the Water-Mediated Reduction of Tris(2,2'-bipyridine-*N,N'*)iron(III), -ruthenium(III), and -osmium(III) Complexes. *Inorg. Chem.* **1985**, *24*, 4707-4710.
- (14) Kotkar, D.; Joshi, V.; Ghosh, P. K. Thermal and Light-Induced Reduction of (+) -Tris(bipyridyl)ruthenium (III) in Aqueous Solution: Mechanistic Inferences from Optical Rotation Studies. *Inorg. Chem.* **1986**, *25*, 4334-4335.
- (15) Serpone, N.; Bolletta, F. On the reduction of trivalent metal-polypyridine complexes by OH⁻ ion in aqueous solutions: An alternative pathway. *Inorg. Chim. Acta* **1983**, *75*, 189-192.
- (16) Serpone, N.; Ponterini, G.; Jamieson, M. A.; Bolletta, F.; Maestri, M. Covalent hydration and pseudobase formation in transition metal polypyridyl complexes: Reality or myth?. *Coord. Chem. Rev.* **1983**, *50*, 209-302.
- (17) Valenti, G.; Rampazzo, E.; Kesarkar, S.; Genovese, D.; Fiorani, A.; Zanut, A.; Palomba, F.; Marcaccio, M.; Paolucci, F.; Prodi, L. Electrogenerated chemiluminescence from metal complexes-

based nanoparticles for highly sensitive sensors applications. *Coord. Chem. Rev.* **2018**, 367, 65-81.

(18) Roundhill, D. M. In *Photochemistry and Photophysics of Metal Complexes*; Fackler, J. J. P., Ed.; Plenum Press: New York, **1994**; p 175.